

THE CHARACTERISTICS OF MINING INDUCED STRESS FLUCTUATIONS IN BROKEN ROCK MASS OVER ONE KILOMETER DEEP COAL MINE

by

Cong LI^a, XiangangYIN^{b*}, Jing XIE^a, and Gaoyou PENG^{b*}

^a State Key Laboratory of Hydraulics and Mountain River Engineering,
College of Water Resource and Hydropower, Sichuan University, Chengdu, China

^b Changsha Institute of Mining Research, Changsha, China

Original scientific paper
<https://doi.org/10.2298/TSCI180621119L>

Mine pressure is critical to the safety of working face. Evaluating the working resistance accurately of the stope hydraulic supports is one of the most effective and direct ways to reflect the overall stress characteristics of the roof and the deformation, movement and destruction of overlying strata. Due to the complex breaking form of the roof, the working resistance of the hydraulic supports at different positions of the mining face varies in different ways. One can obtain the pressure of hydraulic support system by pressure monitoring and analyze its fractal characteristics. Through spectrum analysis, a new parameter called accumulation power spectral density is defined which is used to describe the difference of working resistance of stope hydraulic supports. The results show that the fractal dimensions of face-end supports are smaller and face-end supports are unco-ordinated. Through in-situ monitoring, it is found that the mining stress has unstable periodic fluctuation characteristics. The conclusion can provide reference for rational selection and optimization of the similar-mining lay-outs.

Key words: strata behaviors, working resistance, fractal

Introduction

A reliable description of the supports behavior for long wall mining has always been a challenge for rock mechanics researchers and mine planning engineers. It is very important for successfully capturing the dynamic characteristics at high capacity long wall projects to properly optimize supporting parameters. The working resistance of stope hydraulic supports can indirectly reflect the change of overburden pressure on mining face. Due to the roof characteristics and the interactions [1, 2] between the supports and surrounding rock, the mechanical response of the hydraulic supports under different geological conditions will be different. In last decades, many efforts have been devoted. Peng *et al.* [3] put forward a method of optimizing and inverting working resistance based on the roof control effect and work in resistance overrun percentage. Singh and Singh [4] established a numerical modelling approach to predict the progressive caving behavior of strata and performance of powered roof support in a given geo-mining and strata condition. Singh and Singh [5] also developed a criteria for selection of optimal capacity support by integrating the field experience.

* Corresponding author, e-mail: 459496683@qq.com

Experience shows that it does not provide effective means of support specification [6], although the existing approaches devote important contributions to understand the strata-support interactions. Their applicability in Indian geo-mining condition is limited and suffers from considerable error resulting in inconsistency [7]. The difference of hydraulic supports under different positions is also a problem that should be considered during the support selection process. Zhang *et al.* [8] found that with retreating of the working face, average working resistance of the support reflects overall weighting strength, due to the working face's large deflection of middle roof and low supporting strength of face-end support. Wang *et al.* [9] found that the distribution of working resistance was a sine distribution. However, the existing research is often limited to the study on the weighting distance and weighting strength, and only the average value of work resistance is considered. Gao *et al.* [10] found that the average growth rate of the abutment pressure coefficient exhibits a fluctuating stable growth trend as the mining face progresses by field experiments. Therefore, it is neglected that the information during the mining process containing the state changes and fluctuations of the roof, which could really reflect the process of mining-induced stress redistribution. It is necessary to further explore the complex fluctuation behavior of hydraulic supports.

The letter is an attempt to characterize working resistance anisotropy of supports using one single parameter. The working resistance profile and its slope change are expressed by fractal dimensions. This research illustrates the results of the spectral analysis of slope distribution of pressure of supports. Furthermore, a new parameter, referred to as the index for accumulation power spectral density, P^* , is proposed to describe the complex mechanical response process of the support pressure.

Field test design and results

The field test was conducted at working face No. 15-31010 backfill working face in No. 12 coal mine of the China Pingmei Shenma group. The working face is located in No. 1 district of the third level, corresponds to ground elevation from +300 m to +350 m, under-

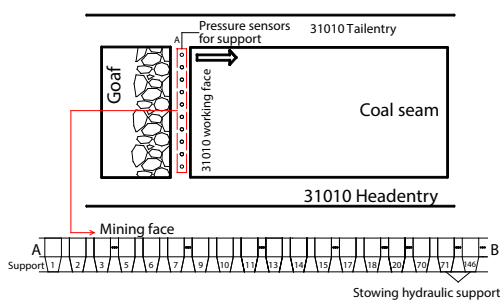


Figure 1. The lay-out drawing of fully mechanized equipment of No. 15-31010 work face

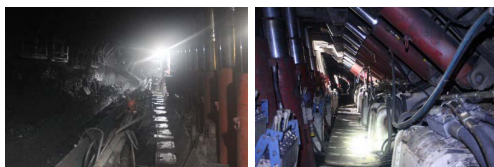


Figure 2. Field photos of the working face of Pingdingshan No. 12 coal mine

ground elevation from -737 m to -806 m, average strike length of 926.2 m, average incline length of 218.5 m, thickness of 3.2 m, average dip angle of 5° . The main roof is a gray-white fine sandstone with a thickness of 2.5 m. The immediate roof is gray sandy mudstone with a thickness of 4.0 m, and the false roof is mudstone with a thickness from 0.5 m to 1.0 m. The ZY6800/20/40 shield hydraulic supports was applied to 31010 working face. The setting load of the supports was 5067 kN. Fifteen observation stations were set up for the working face. The specific lay-out is shown in figs. 1 and 2.

Mine pressure observation lasted about 70 days. The working resistance curves were drawn according to the recorded results, which is partially shown in fig. 3. The results indicated pressure fluctuations as the mining face advanced. The minimum value, the maximum value and the average value of 1[#] support were

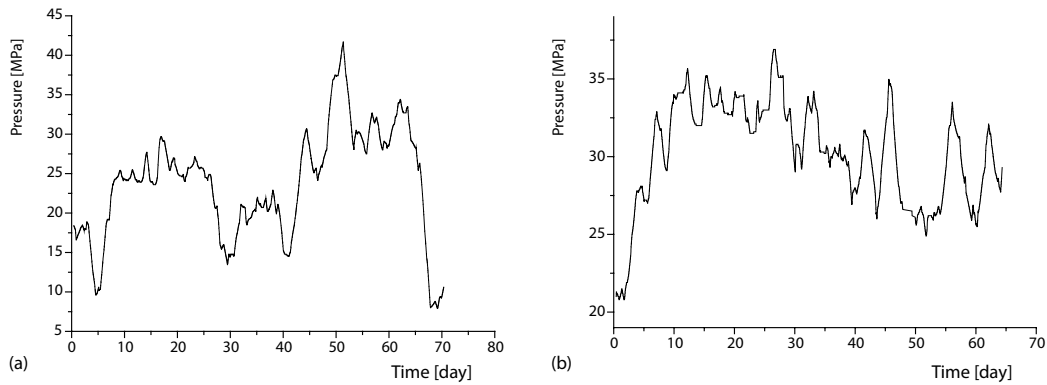


Figure 3. A digitized profile of hydraulic supports; (a) 1# support, (b) 10# support

7.9 MPa, 41.7 MPa, and 23.8 MPa. The minimum value, the maximum value and the average value of supporting pressure of 10# support were 20.8 MPa, 36.9 MPa, and 30.38 MPa. The average pressure of 10# support was greater than the average pressure of 1# support. It can also be seen from the figure that pressure showed obvious cycle characteristics. With the support approaching to the middle working face, the minimum value had an increasing trend, and the maximum value had a decreasing trend, and the average value remained generally stable. According to the criterion of main roof pressure, the main roof periodic pressure step of the 31010 working face was 18.21 m and the first weighting step was 43.2 m with obviously dynamic pressure phenomena. The ratio is pretty close to 2.45 according to the material mechanics which is known to us.

Figure 4 shows the trend of the working resistance of the supports and advancement speed against time. As the speed of advancement increases, there is generally a peak. The working resistance is generally consistent with the advancing speed, indicating that the advancing speed of the mining face has a significant effect on the strata behaviors.

According to fractional Brown function [11], Weierstrass-Mandelbrot fractal function curves [12] and the scanned profile of rock fracture surfaces [13], the pressure curve is consistent with the fractal function curve. Therefore, a similar method can be used to clarify the characteristics of working resistance fluctuations.

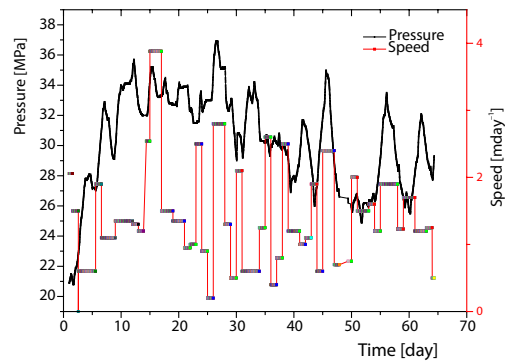


Figure 4. Working resistance and advancing speed of 10# support

Fractal characteristics of results

Considering the pressure changes with time as the input signal in time domain, one can use signal processing methods to discover the rules. It is well known that the spectral analysis is available only for a stationary series, while the pressure distribution is non-stationary, see fig. 3(a), which is similar to the rough surface [14]. It cannot be analyzed with the spectral method directly. Therefore, it is essential to transform a non-stationary series into a stationary

series. For the non-stationary series z_i ($1 < i < N - 1$) composed by the asperity pressure, one may define a new series s_i by:

$$s_i = \frac{z_{i+1} - z_i}{\Delta}, \quad (1 \leq i \leq N - 1) \quad (1)$$

where s_i is a series composed of slope distribution and Δ is the sampling interval. However, the sampling frequency is too dense, and s_i could be defined:

$$s_{i+10} = \frac{z_{i+10} - z_i}{\Delta}, \quad (1 \leq i \leq N - 10) \quad (2)$$

Figure 5 shows the slope of the pressure of 1[#] and 10[#] supports, respectively, which is shown in fig. 3. and fig. 6 suggests that the slope distribution is Gaussian.

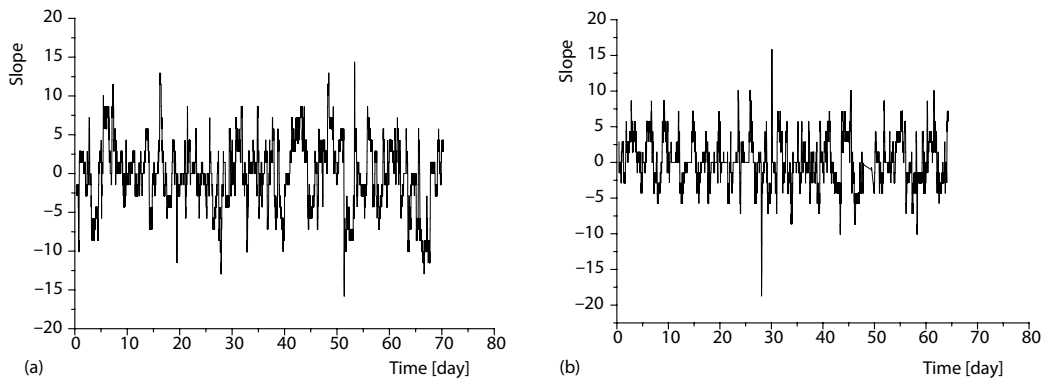


Figure 5. A digitized profile on the slope distribution; (a) 1[#] support, (b) 10[#] support

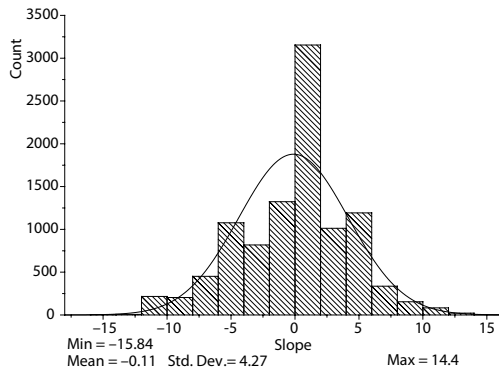


Figure 6. Slope distribution of 1[#] hydraulic support

The auto-correlation function of pressure is defined:

$$ACF(\tau) = \frac{1}{N - j} \sum_{i=1}^{N-j} [z(x_i + \tau) - z(x_i)]^2 \quad (3)$$

where ACF is the auto-correlation function, N – the total number of sampling points, j – the iterate number, τ – the lag distance of two points. The ACF of asperity slope is defined:

$$ACF(\tau) = \frac{1}{N - j} \sum_{i=1}^{N-j} [s(x_i + \tau) - s(x_i)]^2 \quad (4)$$

Based on the data set of figs. 3 and 5, one may obtain the relationship between the ACF and the lag distance, as shown in fig. 7. It is also indicated that the ACF depends only on the lag distance. The pressure distribution is auto-correlated, fig. 7(a), while when the lag distance is ten times more than the sampling interval Δ , the slope distribution is no longer auto-correlated, fig. 7(b).

Structure function method [15] considers the slope profiles as a time series. It is widely used to describe rough surfaces with statistical affine fractal characteristics. The pressure series are naturally a time series. Consequently, the series could be analyzed in the same way.

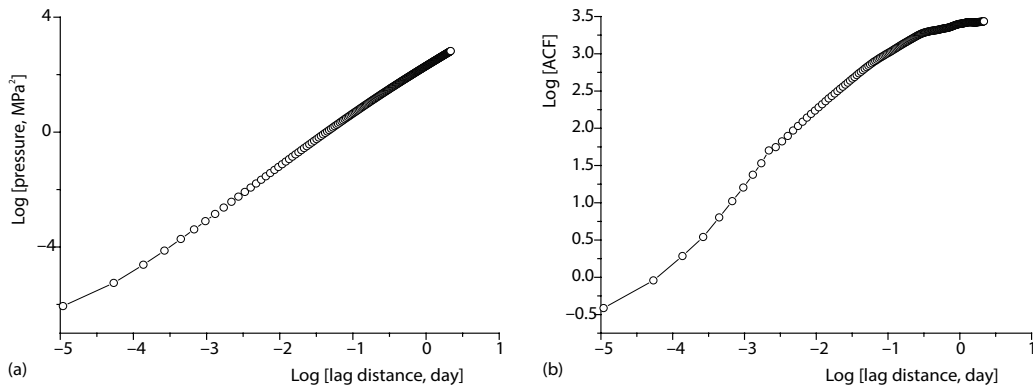


Figure 7. Log-log plot of the ACF and the lag distance correspond with; (a) pressure, (b) slope

Fractal dimension provides a description of how much space a set fill [16]. It is a measure of the prominence of the irregularities of a set when viewed at very small scales. Consider a single valued function of a variable $z(x)$, which satisfies the two features: random aspect and structural aspect. The value of $z(x)$ for a real pressure profile changes with x in a random way.

The variance formulates fractal behavior in the form:

$$V(x) = \langle |z(x_2) - z(x_1)|^2 \rangle \propto |x_2 - x_1|^{2H} \quad (5)$$

where the brackets $\langle \bullet \rangle$ denote average over many samples of $z(x)$, H – the affine exponent.

For a single valued function $z(x)$, the fractal dimension $D = 2 - H$ which has been proven [17, 18]. The variance can be expressed by:

$$V(r) = Ar^\alpha \quad (6)$$

where V is the variance formulates fractal behavior, A – the intercept on V -axis of the log-log plot, α – the slope of the plot. Fractal dimension is thus calculated by:

$$D = 2 - \frac{\alpha}{2} \quad (7)$$

where D is the fractal dimension.

According to eq. (7), the fractal dimensions of supporting pressure and slope at different positions are drawn in fig. 8. Fractal dimension, D , can quantitatively describe the complex-

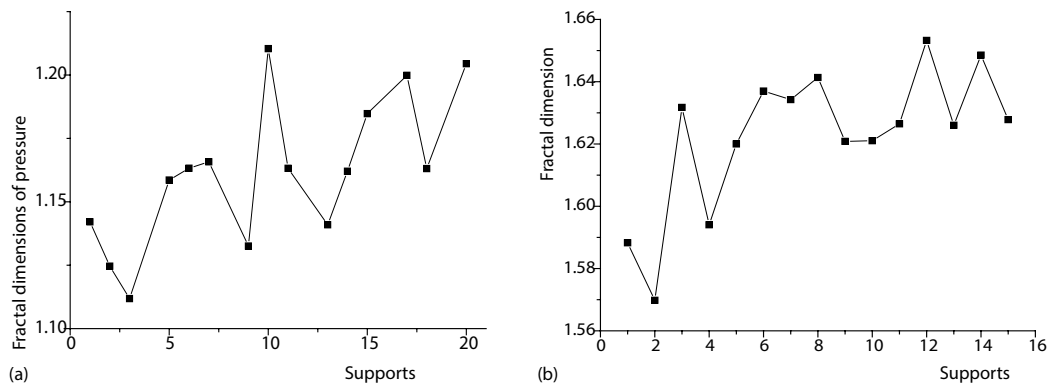


Figure 8. Fractal dimensions of different supports with; (a) pressure, (b) slope

ity of the supporting pressure. A rougher curve with a higher fractal dimension is superimposed by some higher orders of asperities. This can indirectly reflect the period, amplitude and others of the stress redistribution about the roof. The larger the fractal dimension is, the more active the roof is. There is a large difference in fractal dimensions of face end supports, reflecting the unco-ordinated fluctuation of the adjacent supports.

Spectral analysis of working resistance

Spectral analysis provides an effective tool for the understanding the frequency components of the working resistance. It has been successfully applied in other fields such as the broad bandwidth of the topography of natural rock surface [19]. The basis of spectral analysis is to transform a process or a series in a spatial domain into a process or a series in a frequency domain. In this process, MATLAB, a well-known software, is employed to carry out the spectral analysis. The plots of the power spectral density of the profiles with slope of 1[#] and 10[#] supporting pressure against frequencies are depicted in fig. 9.

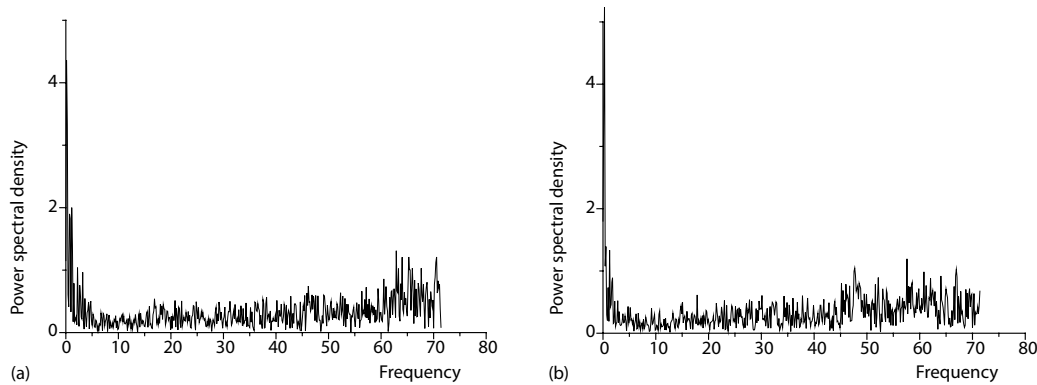


Figure 9. Power spectral density of the profiles with; (a) 1[#] support, (b) 10[#] support

Figure 9 shows that the power spectral densities of slope distribution of profiles are composed of spectrum with different frequencies. Both 1[#] and 10[#] supports have a similar progress. The 1[#] support is larger than the 10[#] support at low frequency section, while the 10[#] support is more concentrated in the intermediate frequency section. It is indicated that the waviness components of pressure, from the perspective of spectrum analysis, has a great influence on the working resistance, which is related to the stress fluctuation of roof. In order to characterize the difference in fig. 9, the vertical co-ordinates are transformed into a new variable which is accumulation power spectral density. It could be obtained by summing up the power spectral density along the frequency axis. Then the power spectral density can be illustrated by a single-valued curve through a plot of accumulation power spectral density against frequencies, as shown in fig. 10.

Figure 10 indicates that both the plots of accumulation power spectral density against frequency, corresponding with the supports of 1[#] and 10[#], respectively, appear to be similar. But the ratio of accumulation power spectral density to whole spectral density in lower frequencies, 1[#] is greater than 10[#]. When the frequency exceeds a certain value, the overall amplitude is less than that of 10[#]. To distinguish the difference, the following parameter is defined by eq. (8).

$$P^* = \sum_{f=MF/3}^{MF} psd \left[\sum_{f=0}^{MF} psd \right]^{-1} \quad (8)$$

where P^* is the index for the accumulation power spectral density, MF – the maximum frequency, psd – the power spectral density. The results in fig. 9 can also be redrawn as a variation of P^* with supports in different positions, as shown in fig. 11.

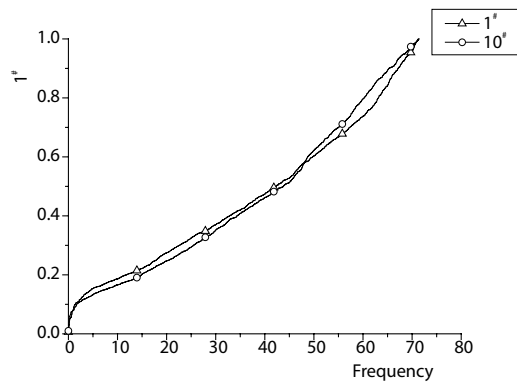


Figure 10. Accumulation power spectral density

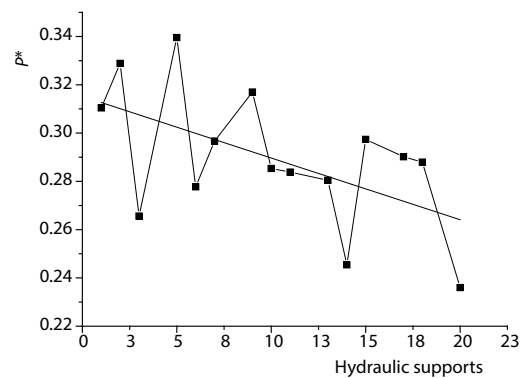


Figure 11. The P^* with different supports

In fig. 11, P^* fluctuates greatly, which probably means that the stress fluctuations at different positions of the roof are quite different. The small P^* indicating that it is concentrated in the high frequency range which means it has a significant fluctuation characteristic. Some values are relatively big, indicating slight fluctuations, but it may also be caused by the lack of close contact between the supports and the roof. As the supports approached to the middle, the P^* decreased generally, which means the pressure is changing frequently.

Discussion and conclusions

The pressure changes of the hydraulic support located at different positions of the working face are quite different. From the end of the 31010 working face to the middle, the accumulation power spectral density of the hydraulic support decreases overall, potentially indicating that working resistance of the middle supports changes dramatically. On the one hand, there is a significant difference among the end supports. It may be that some supports do not have a close contact with the immediate roof, causing a failure to reflect the real situation of the roof. In this case, the mining induced stress fluctuations in broken rock mass can be quantitatively characterized. On the other hand, the P^* of supports 10[#], 11[#], 13[#] and 15[#], 17[#], 18[#] are relatively stable, showing that the supports form an effective support as a whole. In order to further study the wider significance of P^* , it is expected that a large number of data will be used to study its relationship with periodic weighting of main roof.

The mining-induced stress is fluctuant, not static. Conventional methods are difficult to describe the complicated process of work resistance. Observation of working resistance of hydraulic supports for 31010 working face are carried out. The results can be summarized.

- There is a slight difference from the predecessors' theory that is the first weighting step is 2.45 times the length of the periodic weighting step. It means the theory is still applicable for the No. 31010 working face. However, the working face has a strong dynamic pressure phenomenon. According to the measured results of the No. 31010 working face, a fast advance speed is often accompanied by a severe mine pressure appearance.
- Using fractal dimensions to describe the changing characteristics of working resistance. From the end to the middle area at the working face, the fractal dimensions of the support

have an increasing trend. The fractal dimensions represent the frequency of roof activity. In the working face, the face end supports have a smaller fractal dimensions, showing that the roof in that area is more stable.

- The changes of working resistance of supports are analyzed by spectrum analysis. A new method for quantitative description of the working resistance fluctuation process is presented, which could reflect the fluctuation effect of the broken roof as well. As a consequence, the p^* of supports in 31010 working face shows a downward trend. This may indicate that the changes of the middle roof are more complex and intense.

Acknowledgment

This work was financially supported by National Natural Science Foundation of China (Grant No. 51822403 and 51674170).

Nomenclature

A	– intercept on V -axis of the log-log plot
D	– fractal dimension
f	– frequency, [Hz]
H	– affine exponent
j	– iterate number
N	– total number of sampling points
P^*	– index for the accumulation power spectral density
s_p, s_{i+10}	– a series composed of slope distribution
V	– variance formulates fractal behavior
z	– non-stationary series

Greek symbols

α	– slope of the plot
Δ	– sampling interval
τ	– lag distance of two points

Acronyms

ACF	– auto-correlation function
MF	– maximum frequency, [Hz]
psd	– power spectral density

References

- [1] Wang, Z. T., Qian, M. G., The Calculating Methods of the First Weighting Span of Main Roof, *Journal of China University of Mining and Technology* (in Chinese), 18 (1989), 2, pp. 9-18
- [2] Qian, M. G., *et al.*, Research on the Coupling Mechanism between the Stope Support and Surrounding Rock, *Journal of China Coal Society* (in Chinese), 21 (1996), 1, pp. 40-44
- [3] Huang, P., *et al.*, Optimization and Practice of Support Working Resistance in Fully-Mechanized Top Coal Caving in Shallow Thick Seam, *Energies*, 10 (2017), 9, 1406
- [4] Singh, G. S. P., Singh, U. K., A Numerical Modelling Approach for Assessment of Progressive Caving of Strata and Performance of Hydraulic Powered Support in Longwall Workings, *Computers and Geotechnics*, 36 (2009), 7, pp. 1142-1156
- [5] Singh, G. S. P., Singh, U. K., Prediction of Caving Behavior of Strata and Optimum Rating of Hydraulic Powered Support for Longwall Workings, *International Journal of Rock Mechanics and Mining Sciences*, 47 (2010), 1, pp. 1-16
- [6] Trueman, R., *et al.*, Assessing Longwall Support-roof Interaction from Shield Leg Pressure Data, *Mining Technology*, 114 (2005), 3, pp. 176-184
- [7] Sarkar, S. K., Singh, B., The Investigation into Strata Control Failures at Caved Longwall Faces in India and a New Approach for Support Planning to Avoid such Occurrences, *Proceedings, Emerging Trends in Engineering & Technology, International Conference on IEEE*, 1979, Vol. 105, pp. 468-473
- [8] Zhang Q., *et al.*, Mining Pressure Monitoring and Analysis in Fully Mechanized Backfilling Coal Mining Face-A Case Study in Zhai Zhen Coal Mine, *Journal of Central South University*, 22 (2015), 5, pp. 1965-1972
- [9] Wang Z., *et al.*, Measurement of the Strong Pressure Appearance Laws with Hard Roof and Full Mechanized Mining Extra Thick Coal Seam, *Geotechnical and Geological Engineering*, 36 (2018), 6, pp. 3399-3409
- [10] Gao, M.Z., *et al.*, Field Experiments on Fracture Evolution and Correlations between Connectivity and Abutment Pressure under Top Coal Caving Conditions. *International Journal of Rock Mechanics and Mining Science*, 111 (2018), Oct., pp. 84-93

- [11] Mandelbrot, B. B., Freeman, W. H., *The Fractal Geometry of Nature*, W. H. Freeman and Company, 1983, Vol. 51
- [12] Berry, M. V., Lewis, Z. V., On the Weierstrass-Mandelbrot Fractal Function, *Proceedings of the Royal Society of London*, 370 (1980), 1743, pp. 459-484
- [13] Zhou, H. W., Xie, H., Anisotropic Characterization of Rock Fracture Surfaces Subjected to Profile Analysis, *Physics Letters A*, 325 (2004), 5-6, pp. 355-362
- [14] Sayles, R. S., Thomas, T. R., Surface Topography as a Non-stationary Random Process, *Nature*, 271 (1978), 5644, pp. 431-434
- [15] Ge, S. R., Zhu, H., *Fractal in Tribology* (in Chinese), China Machine Press, Beijing, China, 2005
- [16] Xie, H. P., *et al.*, Fractal Effects of Surface Roughness on the Mechanical Behavior of Rock Joints, *Chaos Solitons and Fractals*, 8 (1997), 2, pp. 221-252
- [17] Feder, J., *Fractals*, Plenum Press, New York, USA, 1988
- [18] Falconer, K. J., Fractal Geometry – Mathematical Foundations and Applications, *Biometrics*, 46 (1990), 3, 499
- [19] Brown, S. R., Scholz, C. H., Broad Bandwidth Study of the Topography of Natural Rock Surfaces, *Journal of Geophysical Research Solid Earth*, 90 (1985), B14, pp. 12575-1258